

Kinetic accumulation processes and models for 43 micropollutants in "pharmaceutical" POCIS

Nicolas A.O. Morin, Nicolas Mazzella, Hans Peter H. Arp, Jérôme Randon, Julien Camilleri, Laure Wiest, Marina Coquery, Cecile Miege

▶ **To cite this version:**

Nicolas A.O. Morin, Nicolas Mazzella, Hans Peter H. Arp, Jérôme Randon, Julien Camilleri, et al.. Kinetic accumulation processes and models for 43 micropollutants in "pharmaceutical" POCIS. Science of the Total Environment, 2018, 615, pp.197-207. 10.1016/j.scitotenv.2017.08.311 . hal-02119712

HAL Id: hal-02119712
https://hal.science/hal-02119712

Submitted on 4 Oct 2021

HAL is a multi-disciplinary open access archive for the deposit and dissemination of scientific research documents, whether they are published or not. The documents may come from teaching and research institutions in France or abroad, or from public or private research centers.

L'archive ouverte pluridisciplinaire **HAL**, est destinée au dépôt et à la diffusion de documents scientifiques de niveau recherche, publiés ou non, émanant des établissements d'enseignement et de recherche français ou étrangers, des laboratoires publics ou privés.



Distributed under a Creative Commons Attribution 4.0 International License

Kinetic accumulation processes and models for 43 micropollutants in "pharmaceutical" POCIS

Nicolas A.O. Morin [a,1], Nicolas Mazzella [b], Hans Peter H. Arp [c], Jérôme Randon [d], Julien Camilleri [d], Laure Wiest [d], Marina Coquery [a], Cécile Miège [a,*]

[a] *Irstea, UR MALY, Centre de Lyon-Villeurbanne, 5 rue de la Doua, CS 20244, F-69625 Villeurbanne Cedex, France*
[b] *Irstea, UR EABX, Centre de Bordeaux, 50 avenue de Verdun, F-33612 Cestas Cedex, France*
[c] *Norwegian Geotechnical Institute (NGI), P.O. Box 3930, Ullevål Stadion, 0806 Oslo, Norway*
[d] *Institute of Analytical Sciences (ISA), UMR CNRS 5280, University Claude Bernard Lyon I, 5 rue de la Doua, 69100 Villeurbanne, France*

The "pharmaceutical" polar organic integrative sampler (POCIS) is a passive sampler composed of an outer polyethersulfone (PES) membrane and an inner receiving Hydrophilic-Lipophilic Balance (HLB) phase. Target micropollutants can accumulate in the POCIS HLB phase following different uptake patterns. Two of the most common ones are a first-order kinetic uptake (Chemical Reaction Kinetic 1, CRK1 model), and a first-order kinetic uptake with an inflexion point (CRK2 model). From a previous study, we identified 30 and 13 micropollutants following CRK1 and CRK2 accumulation model in the POCIS HLB phase, respectively. We hypothesized that uptake in the outer PES membrane of POCIS may influence the uptake pathway. Thus, novel measurements of uptake in PES membrane were performed for these micropollutants to characterise kinetic accumulation in the membrane with and without the HLB phase. We determined, for the first time, the membrane-water distribution coefficient for 31 micropolluants. Moreover, the lag times for molecules to breakthrough the POCIS membrane increased with increasing hydrophobicity, defined by the octanol-water dissociation constant D_{ow}. However, D_{ow} alone was insufficient to predict whether uptake followed a CRK1 or CRK2 model in the POCIS HLB phase. Thus, we performed a factorial discriminant analysis considering several molecular physico-chemical properties, and the model of accumulation for the studied micropollutants can be predicted with >90% confidence. The most influent properties to predict the accumulation model were the log D_{ow} and the polar surface area of the molecule (>70% confidence with just these two properties). Molecules exhibiting a CRK1 uptake model for the POCIS HLB phase tended to have log $D_{ow} > 2.5$ and polar surface area <50 Å^2.

* Corresponding author.
E-mail address: cecile.miege@irstea.fr (C. Miège).
[1] Present address: Environmental and Food Laboratory of Vendée (LEAV), Department of Chemistry, Rond-point Georges Duval CS 80802, 85021 La Roche-sur-Yon, France.

1. Introduction

Passive samplers are useful tools for the measurement of organic micropollutant concentrations in surface waters. These devices are usually exposed in natural or waste waters for periods from a few days to several weeks, during which they accumulate micropollutants by passive uptake. In the simplest case, accumulation in passive samplers follows a first-order kinetic pathway (Vrana et al., 2005), which can be subdivided into three regimes, first linear accumulation, then curvilinear accumulation, and finally equilibrium. If passive samplers are used in the linear accumulation regime they are referred to as integrative samplers, while in the equilibrium regime they are referred to as equilibrium samplers. Integrative samplers can be used to determine time-weighted average (TWA) concentrations, and thus are more appropriate than equilibrium samplers in areas where water concentrations vary with time. Passive samplers are generally able to decrease limits of quantification in comparison to classical grab water sampling (Morin et al., 2012). Different types of passive samplers have been developed according to the nature of organic micropollutant studied (Seethapathy et al., 2008). For hydrophilic molecules, the Polar Organic Chemical Integrative Sampler (POCIS) is often used (Alvarez et al., 2004; Zabiegała et al., 2010). Generally, POCIS is made of a solid receiving phase (a triphasic mixture composed of Isolute ENV+, Ambersorb 1500 and S-X3 Bio-Beads in its "pesticide" configuration or an Oasis® HLB phase in its "pharmaceutical" configuration) sandwiched between 2 polyethersulfone (PES) membranes (0.1 μm pore size). POCIS has been applied for investigating micropollutants in water quantitatively (Lissalde et al., 2011; Mazzella et al., 2007) and qualitatively (Alvarez et al., 2005), as well as in bioaccumulation studies (Vermeirssen et al., 2005).

Quantitative aspects to determine TWA concentrations using POCIS still need further research (Harman et al., 2011; Mills et al., 2014). Uptake is dependent on the materials composing the POCIS (e.g. membrane material, membrane porosity, receiving phase material) (Alvarez, 1999; Belles et al., 2014a; Fauvelle et al., 2012), as well as on several environmental factors like water flow velocities, temperature and biofouling (Morin et al., 2012). In an attempt to account for these variables, the use of performance reference compounds (PRCs) was first proposed for hydrophobic passive samplers (Booij et al., 1998; Huckins et al., 2002). PRCs are "spiked" into the passive sampler prior to deployment. If it can be demonstrated that the desorption of the PRCs and uptake of the target analytes follow a similar (isotropic) kinetic behaviour, then PRC depletion provides a convenient way to account for variability of uptake rates. In theory, this condition can be fulfilled when partitioning (absorption) phenomena are involved, as it is the case for hydrophobic passive samplers. But anisotropic exchanges are expected when using a sorbent receiving phase that involves adsorption phenomena. Sorbent materials are often used in hydrophilic passive samplers, such as POCIS.

Isotropic exchange has been demonstrated for polycyclic aromatic hydrocarbons (PAHs) and polychlorinated biphenyls (PCBs) in passive samplers like SPMD (semi-permeable membrane device), LDPE (low density polyethylene) and SR (silicon rubber) (Booij et al., 1998; Huckins et al., 2002; Rusina et al., 2010). Until now, investigations on POCIS have not indicated if sorption-desorption was isotropic, except for two pesticides, deisopropylatrazine (DIA) and cyanazine (Belles et al., 2014b; Mazzella et al., 2007). The mechanisms involved in desorption are still unclear; thus, the potential for PRCs in POCIS may be limited, leading to TWA concentrations with unknown uncertainty, as recently stated by Miège et al. (2015). Consequently, understanding the uptake mechanisms of polar compounds for adsorption-based passive samplers, such as POCIS, is the most important issue that needs to be resolved. Indeed, this may permit to reduce the currently observed uncertainties in passive sampling data on hydrophilic micropollutants and allow their use for evaluation of quantitative TWA concentrations in various types of waters.

Recent studies showed that a first-order kinetic model did not properly fit the uptake of the most hydrophilic and ionisable molecules (with log $D_{ow} < 1$) in the HLB phase of "pharmaceutical" POCIS (Belles et al., 2014a; Fauvelle et al., 2014; Morin et al., 2013). The HLB sorbent has two different moieties (one apolar: divinylbenzene – DVB, and one polar: N-vinylpyrrolidone – NVP), which might lead to double Langmuir sorption isotherms for some compounds (Bäuerlein et al., 2012; Fauvelle et al., 2014). Thus, currently available models for POCIS are empirical. Further studies, including some on the role of the membrane, are still needed for hydrophilic molecules, to increase knowledge on uptake and release mechanisms and models.

If the distribution of micropollutants in the receiving compartment of a passive sampler is homogeneous and the concentration in the surrounding water compartment is kept constant, first order uptake kinetics can be assumed. First-order kinetics have been showed to successfully describe uptake of hydrophobic compounds in SPMD, LDPE and SR devices (Booij et al., 2003; Huckins et al., 1993; Huckins et al., 1999; Rusina et al., 2010) and of hydrophilic molecules in POCIS (Mazzella et al., 2007). For PAHs and PCBs in SPMD, LDPE and SR, correlations between sampling rates (R_s) and octanol-water distribution coefficients (log K_{ow}) between 3.0 and 7.5 were proposed to approximate R_s (Booij et al., 2003; Huckins et al., 1999; Rusina et al., 2010). In a previous work, we studied the accumulations of 56 relatively polar organic chemicals (hormones, pharmaceuticals, alkylphenols, UV filter, pesticides) in the HLB receiving phase of "pharmaceutical" POCIS using a flow-through calibration system (Morin et al., 2013). We were able to distinguish 4 groups of micropollutants according to the type of accumulation: group 1 consisted of 30 micropollutants with first-order uptake curves (that we classify in the present paper as CRK1, for Chemical Reaction Kinetic 1 model), group 2 consisted of 13 micropollutants with first-order uptake curves though with an inflexion point (classified as CRK2 model in the present paper), group 3 consisted of 8 micropollutants with random accumulations (mainly due to molecule degradation in water) and group 4 consisted of 5 micropollutants with low or no accumulation.

In this work, we tested the hypothesis that uptake kinetics in the POCIS membrane plays a contributing role on whether uptake in the POCIS HLB phase follows a CRK1 or CRK2 model. In this aim, we focused on the 43 micropollutants for which the uptake in "pharmaceutical" POCIS HLB phase was previously characterized (Morin et al., 2013). We measured their uptake in the membrane of a whole "pharmaceutical" POCIS with the HLB phase, and of a "membrane-only" POCIS without the HLB phase. Then, we applied two uptake models from the literature to describe the accumulation curve type (Fauvelle et al., 2014; Vrana et al., 2005). In addition, we used a factorial discriminant analysis (FDA) to identify if micropollutant physico-chemical properties permitted to predict the accumulation type in the POCIS HLB phase.

2. Theory: accumulation models for "pharmaceutical" POCIS

Accumulation of a compound from water into a receiving medium can be described by Fick's first law of diffusion, assuming linear

concentration gradients between the layers separating external bulk water and the receiving medium (Górecki and Namienik, 2002). This diffusion can be parameterized with a mass-transfer coefficient (MTC) model that is based on mathematical description of solute-mass transfer (fluxes) through the different boundary layers. In the case of a simple boundary layer between water and membrane, Fick's first law can be expressed as Eq. (1):

$$j_i = k_i(C_{i+} - C_{i-}) \quad (1)$$

where j_i is the flux of a molecule through a boundary layer (μg/cm^2/s), k_i is the mass transfer coefficient of a molecule through a boundary layer (cm/s), C_{i+} is the concentration of a molecule on one side of the boundary layer (μg/L) and C_{i-} is the concentration of a molecule on the other side of the boundary layer (μg/L).

In the case of "pharmaceutical" POCIS, when the micropollutant concentration in the membrane is reaching a steady-state, the overall flux is expressed by Eq. (2), assuming that the fluxes are homogenous in water and for each POCIS layer and that sorption equilibrium exists at all interfaces (including the membrane) (Huckins et al., 2006):

$$j = k_0\left(C_w - \frac{C_{HLB}}{K_{HLBw}}\right) \quad (2)$$

where j is the overall flux of a micropollutant from water into POCIS (μg/cm^2/s), k_0 is the overall mass transfer coefficient for uptake into the POCIS (cm/s), C_w is the concentration of micropollutant in the bulk water (μg/L), C_{HLB} is the concentration of micropollutant in the POCIS HLB phase (μg/g) and K_{HLBw} is the HLB-water distribution coefficient (L/g).

The concentration of micropollutant in the POCIS HLB phase, as a function of time, can be calculated as follows:

$$\frac{dC_{HLB}}{dt} = \frac{Aj}{M_{HLB}} = \frac{Ak_o}{M_{HLB}}\left(C_w - \frac{C_{HLB}}{K_{HLBw}}\right) \quad (3)$$

where A is the membrane surface area (cm^2), M_{HLB} is the mass of HLB phase (g), and j is the flux from Eq. (2).

In "pharmaceutical" POCIS, 3 different boundary layers are expected, assuming that the biofouling layer is negligible (Alvarez et al., 2004): the water-boundary layer (WBL), the membrane layer and the HLB-boundary layer. Therefore, the inverse of k_o, which represents the overall mass-transfer resistance in the POCIS (s/cm), is an addition of each mass-transfer resistance layer, as presented in Eq. (4). This is referred to, in the present paper, as the MTC_m model:

$$MTC_m \quad \frac{1}{k_o} = \frac{1}{k_w} + \frac{1}{k_m K_{mw}} + \frac{1}{k_{HLB} K_{HLBm}} = \frac{\delta_w}{D_w} + \frac{\delta_m}{D_m K_{mw}} + \frac{\delta_{HLB}}{D_{HLB} K_{HLBm}} \quad (4)$$

where $1/k_w$ is the WBL mass-transfer resistance (s/cm), $1/k_m$ is the membrane mass-transfer resistance (s/cm), K_{mw} is the membrane-water distribution coefficient (L/g), $1/k_{HLB}$ is the HLB mass-transfer resistance (s/cm) and K_{HLBm} is the HLB-membrane distribution coefficient (L/g). δ represents the thickness of a particular layer (cm) and D the diffusivity coefficient of a micropollutant in a particular layer (cm^2/s), with w for water, m for the membrane and HLB for the HLB phase (Vermeirssen et al., 2012).

For micropollutants that do not have substantial affinity to the membrane and predominately transfer through the membrane pores as described by Kaserzon et al. (2014) or Booij et al. (2017), the mass-transfer resistance into the POCIS can be described with a modified version of Eq. (4) to obtain Eq. (5):

$$MTC_p \quad \frac{1}{k_o} = \frac{1}{k_w} + \frac{1}{k_p K_{mp}} + \frac{1}{k_{HLB} K_{HLBp}} = \frac{\delta_w}{D_w} + \frac{\delta_m \tau^2}{D_w \phi} + \frac{\delta_{HLB}}{D_{HLB} K_{HLBp}} \quad (5)$$

where $1/k_p$ is the water filled pore mass-transfer resistance (s/cm), δ_m the membrane thickness (cm), τ and ϕ the tortuosity and their porosity factors, respectively. K_{mp} is the distribution coefficient (L/g) of each micropollutant between the water filled pores and the membrane surface, K_{HLBp} is the HLB-water filled pore membrane distribution coefficient (L/g).

The terms K_{HLBm} and K_{HLBp} in Eqs. (4) and (5) are simplified and globalised: they take into account the distribution between the inner water within the HLB phase and the HLB phase itself.

However, a control by the water boundary layer was generally shown (Alvarez et al., 2004). The use of Eqs. (4) and (5) is meant to refine the model as it allows to also differentiate micropollutants controlled either by the membrane or the HLB phase (depending on the relative predominance of terms $1/(k_m K_{mw})$ (or $1/(k_p K_{mp})$), and $1/(k_{HLB} K_{HLBm})$ (or $1/(k_{HLB} K_{HLBp})$).

The first-order CRK1 accumulation mode can be modeled by solving Eq. (3) (Alvarez, 1999), assuming the initial condition of $C_{POCIS} = 0$ at $t = 0$, that micropollutants are well mixed in the HLB once they are introduced, and that their water concentrations remain constant, as expressed in the following CRK1 model Eq. (6):

$$\text{CRK1 model}: CF_{HLB} = \frac{C_{HLB}}{C_w} = K_{HLBw}\left(1 - e^{-k_e t}\right) = \frac{k_u}{k_e}\left(1 - e^{-k_e t}\right) \quad (6)$$

where CF_{HLB} is the concentration factor in the POCIS HLB phase (L/g), k_u the accumulation rate constant of the micropollutant in the POCIS HLB phase (L/g/d), k_e the elimination (or exchange) rate constant of the micropollutant in the POCIS HLB phase (1/d) and t the exposure time (d). An analogous equation can be made for $CF_{membrane}$.

In cases where this CRK1 model fits the uptake data of a micropolluant, it is likely that one type of first-order uptake process dominates over time.

However, with solid receiving phase, multiple interactions can occur and therefore, a main kinetic relationship with several parallel first-order uptake processes are used to describe the system (Fauvelle et al., 2014), as proposed in the following CRK2 model:

$$\text{CRK2 model}: CF_{HLB} = \sum K_{HLB\ w(i)}\left(1 - e^{-k_{e(i)} t}\right) \quad (7)$$

where (i) represents various main interaction phenomena between the POCIS HLB phase and the micropollutants. However, as in our previous work (Morin et al., 2013) we observed a linear accumulation kinetic after the inflexion point (i.e. equilibrium was not reached for the second exponential term), so Eq. (7) can be simplified empirically to Eq. (8):

$$CF_{HLB} = K_{HLB\ w1}\left(1 - e^{-k_{e1} t}\right) + k_{u2} t = \frac{k_{u1}}{k_{e1}}\left(1 - e^{-k_{e1} t}\right) + k_{u2} t \quad (8)$$

where the subscripts 1 and 2 refer to the first-order and the linear types of accumulation, respectively.

There are various scenarios that could explain CRK2 model accumulation in the "pharmaceutical" POCIS. In the membrane, two modes of sorption could occur sequentially: fast sorption to macropores followed by slow sorption to mesopores and micropores (Belles et al., 2014a; Górecki et al., 1999; Rafferty et al., 2007), or fast sorption followed by slow absorption (Belles et al., 2014a). Different uptake regimes dominating over time could also occur for the HLB phase layer. In addition, as the HLB phase consists of N-vinylpyrolidone and polystyrene divinylbenzene groups (Bäuerlein et al., 2012), if some subgroups become saturated quicker than others, changes in uptake rates could occur over time.

With the CRK1 model, it is possible to link the concentration factor to the so-called sampling rates (R_s) using Eq. (9):

$$CF_{HLB} = \frac{R_s t}{M_{HLB}} \quad (9)$$

where R_s is the sampling rate of a micropollutant in the POCIS (L/d).

Moreover, using the CRK1 model it is also possible to determine the $t_{1/2}$, which corresponds to the time needed for reaching half of the equilibrium micropollutant concentration. It is defined by Eq. (10):

$$t_{1/2} = \frac{\ln 2}{k_e} \quad (10)$$

$t_{1/2}$ can be defined as a "frontier" between the integrative and the curvilinear regime.

In contrast, with the CRK2 model, R_s and $t_{1/2}$ cannot be determined.

3. Material and methods

The micropollutants selected, the analytical method used as well as the calibration system and the sample preparation have been described in details previously (Morin et al., 2013; Camilleri et al., 2012; Gabet-Giraud et al., 2010; Miège et al., 2009), and are only briefly presented in the next sections.

3.1. Micropollutants and description of the analytical methods

The 43 micropollutants studied in this paper, classified by family, as well as their respective analytical method are indicated in Table 1. The 30 micropollutants in italic characters were previously reported to belong to group 2 (CRK2 model), and the 10 other micropollutants to group 1 (CRK1 model), considering the POCIS HLB phase (Morin et al., 2013). All the micropollutants were analysed using a liquid chromatography coupled with a tandem mass spectrometer in a positive (LC-ESI(+)-MS/MS) or a negative electrospray mode (LC-ESI(−)-MS/MS).

Analytical methods used for 10 beta-blockers and 5 estrogens are detailed elsewhere (Gabet-Giraud et al., 2010; Miège et al., 2009). Briefly, the analysis system consisted of an Agilent 1100 chromatographic system coupled with an API 4000 triple-quadrupole mass spectrometer from AB Sciex. Separation was performed with Xbridge C18 end-capped columns (150 × 2.1 mm, 3.5 μm) equipped with guard columns and using gradients with LC-MS grade water (buffered with ammonium formiate for beta-blockers) and acetonitrile. Mass spectrometry was performed with an electrospray in positive mode for beta-blockers and in negative mode for estrogens.

The multiresidue methods used for the other 28 micropollutants are described elsewhere (Camilleri et al., 2012; Morin et al., 2013). Briefly, the analysis system consisted of an Agilent 1200 chromatographic system coupled with a triple-quadrupole 3200 Qtrap from AB Sciex. The chromatographic column used for separation was a Kinetex XB-C18 Core Shell (100 × 2.1 mm, 1.7 μm) equipped with a KrudKatcher (0.2 μm) filter. In positive mode (for 21 molecules, including the UV filter, 3 hormones other than estrogens, all pesticides except 2.4-dichlorophenoxyacetic acid, and almost all pharmaceuticals except furosemide and ibuprofene), the separation was performed with a multi-linear gradient with water (acidified with formic acid) and acetonitrile. In negative mode (for 7 molecules, including all alkylphenols and phenols, 2.4-dichlorophenoxyacetic acid, furosemide and ibuprofene), the separation was done with a multistep gradient with 0.1 mM ammonium acetate in water and acetonitrile.

3.2. POCIS

"Pharmaceutical" POCIS was constructed in house using Oasis® HLB bulk sorbent as the receiving phase (200 ± 5 mg, 60 μm particle size), and two membranes of hydrophilic polyethersulfone (PES, SUPOR 100 membrane disc filters, 90 mm diameter, 45.8 cm^2 of exposed surface, 0.1 μm pore size). This type of POCIS was preferred to the "pesticide" POCIS because it was easier to use (less static, more wettable and easier to transfer into SPE cartridges).

Table 1
The 43 micropollutants studied, classified by family, and their respective analytical method. Micropollutants in italic characters were previously reported to belong to group 2 (CRK2 model) while other micropollutants to group 1 (CRK1 model), considering the POCIS HLB phase (Morin et al., 2013).

Family of micropollutant (Number of micropollutant(s))	Micropollutant	Analytical method
Alkylphenols and phenols (n = 4)	Bisphenol A [BPA], t-Butylphenol [t-BP], 2.4-Dichlorophenol-d3 [2.4-DCP], t-Octylphenol [t-OP]	Method 4[d]
Antibiotics (n = 2)	*Sulfamethoxazole* [*Sulfa*], *Trimethoprim* [*Trim*]	Method 3[c]
Anti-inflammatories (n = 4)	Diclofenac [Diclof], *Ibuprofene* [*Ibu*], *Ketoprofene* [*Keto*], *Naproxene* [*Napro*]	Method 3[c] Method 4 for Ibu[d]
Benzodiazepines (n = 2)	Lorazepam [Lora], Oxazepam [Oxa]	Method 3[c]
Beta-blockers (n = 10)	Acebutolol [Ace], *Atenolol* [*Ate*], Betaxolol [Bet], Bisoprolol [Bis], Metoprolol [Met], *Nadolol* [*Nad*], Oxprenolol [Oxp], Propranolol [Prop], *Sotalol* [*Sot*], Timolol [Tim]	Method 1[a]
Lipopenic (n = 1)	*Bezafibrate* [*Beza*]	Method 3[c]
Antiepileptic (n = 1)	Carbamazepine [Carba]	Method 3[c]
Diuretic (n = 1)	*Furosemide* [*Furo*]	Method 4[d]
Fungicides (n = 2)	*Carbendazim* [*Carb*], Prochloraz [Pro]	Method 3[c]
Herbicides (n = 7)	*2.4-Dichlorophenoxyacetic acid* [*2.4-D*], 3.4-Dichloroaniline [3.4-D], Acetochlore [Acet], Alachlore [Ala], Atrazine [Atra], Diuron [Diu], Linuron [Lin]	Method 3[c] Method 4 for 2.4-D[d]
Estrogens (n = 5)	Estrone [E1], 17α-Estradiol [α-E2], 17β-Estradiol [β-E2], *Estriol* [*E3*], Ethynilestradiol [EE2]	Method 2[b]
Progestogens (n = 2)	Megestrol [MegA], Progesterone [P]	Method 3[c]
Androgen (n = 1)	Testosterone [T]	Method 3[c]
UV filter (n = 1)	4-Methylbenzylidene camphor [4-MBC]	Method 3[c]

[a] Method 1: LC-ESI(+)-MS/MS (Agilent 1100-AB Sciex API 4000).
[b] Method 2: LC-ESI(−)-MS/MS (Agilent 1100-AB Sciex API 4000).
[c] Method 3: LC-ESI(+)-MS/MS (Agilent 1200-AB Sciex API 3200).
[d] Method 4: LC-ESI(−)-MS/MS (Agilent 1200-AB Sciex API 3200).

3.3. Calibration system

The calibration system consisted of two aquaria (50 L each) filled by tap water freshly spiked with 3 μg/L of each micropollutant. It was a flow-through calibration system: a freshly-spiked tap water was delivered continuously into each aquarium using a peristaltic pump (the excess was evacuated via an overflow). Triplicates of "pharmaceutical" POCIS were exposed and collected at t = 1, 3, 6 and 12 h and at t = 1, 3, 7, 14, 21 and 28 days. Unique to this study, triplicates of "membrane-only" POCIS (i.e. POCIS without the HLB phase) were immersed for 7 days. During calibration, physico-chemical parameters (temperature, pH, conductivity, dissolved organic carbon, flow velocities) and water micropollutant concentrations were controlled once a week to

ensure they stayed relatively constant with time. Relative standard deviations (RSDs) were <30% for the physico-chemical parameters and <35% for the water micropollutant concentrations (except for t-butylphenol, progesterone and 4-methylbenzylidene camphor with RSD <50%). We used concentration factors (CF) in the POCIS HLB phase (CF_{HLB}) and in the POCIS membrane ($CF_{membrane}$) for data treatment and interpretations, in order to take into account these water concentration variations. The concentration factor, which is also referred to as an uptake quotient, is equal to the ratio of micropollutant concentration in the compartment considered (POCIS HLB phase C_{HLB} or POCIS membrane $C_{membrane}$), over micropollutant concentration in water, C_w (e.g. $CF_{HLB} = C_{HLB}/C_w$).

3.4. Pre-treatment of the POCIS HLB phase and POCIS membrane

POCIS were stored at 4 °C before immersion and at −20 °C after immersion and before extraction. We assumed no degradation of the micropollutants studied during the period of storage (Carlson et al., 2013). One fabrication blank POCIS (not immersed) was made and kept at −20 °C until being processed for analysis in order to check for possible contamination.

Exposed and blank POCIS were left at ambient temperature for 1 h before processing. POCIS HLB phase samples were transferred with a few milliliters of ultrapure water in pre-weighted 6 mL glass solid phase extraction cartridges equipped with polytetrafluoroethylene frits. POCIS membranes were rinsed with ultrapure water and dried with absorbent paper for 30 min. Then, they were rolled and placed into test tubes. The POCIS HLB phase was eluted with 2 × 5 mL of methanol and then with 2 × 5 mL of a mixture methanol/dichloromethane (50/50, v/v). The membranes were extracted with 14 mL of methanol and then 12 mL of a mixture methanol/dichloromethane (50/50, v/v) for 30 min each, using a Syncore Polyvap (Buchi) rotating at 250 rpm. Sorbent and membrane eluates were separated in 3 fractions in order to quantify all the micropollutants using the 4 analytical methods as stated in Table 1. The 3 fractions were evaporated to dryness under a gentle stream of nitrogen. The extracts were then reconstituted into:

- 500 µL (1000 µL for membranes) of a mixture H_2O/ACN (99/1, v/v) including recovery standard at 50 µg/L (i.e. metoprolol impurity A) for beta-blockers analysis (method 1),
- 500 µL (1000 µL for membranes) of a mixture H_2O/ACN (60/40, v/v) including recovery standard at 50 µg/L (i.e. estradiol acetate) for estrogen analysis (method 2),
- 2 mL of a mixture H_2O/ACN (80/20, v/v) for the 2 multiresidue analyses (methods 3 and 4).

For beta-blockers and estrogens, extracts of POCIS membranes were filtered (DCM dissolves PES) through Chromafil polyethylene terephthalate (PET) (0.2 µm, 25 mm diameter). Filtration recoveries were controlled and corrected by the use of solvent spiked at 100 µg/L and filtered through Chromafil PET (mean recoveries were 74% and 90% for beta-blockers and estrogens, respectively). This filtration step was not done for the analyses of the 28 other micropollutants due to the important final dilution factor in ultrapure water (see next paragraph), leading to a relatively clean extract (methods 3 and 4).

Before analysis, extracts were diluted 100 to 500 times in order to be within the concentration range of each chromatographic method and to prevent matrix effects. For beta-blocker and estrogen analyses, dilutions were done in their respective mobile phase mixtures. For multi-residue analyses, extracts were diluted in ultrapure water. All the extracts were stored at −20 °C until analysis by LC-MS/MS.

3.5. Pre-treatment of water samples

Water samples were analysed by direct injection after moderate dilution to obtain the adequate mobile phase mixture (i.e. H_2O/ACN (99/1, v/v) for beta-blockers, H_2O/ACN (60/40, v/v) for estrogens, and ultrapure water for multi-residue analyses), after the addition of eventual recovery standards (metoprolol impurity A and estradiol acetate at 50 µg/L for beta-blockers and estrogens, respectively). Regarding the analyses of the 28 other micropollutants (methods 3 and 4), a study was done following ICH recommendations to validate the direct injection of water samples. Water samples were kept at −20 °C until LC-MS/MS analysis.

3.6. Factorial discriminant analysis (FDA)

Factorial discriminant analysis (FDA) at the 5% significance level ($\alpha = 0.05$) was performed using XLStat Software (Addinsoft). FDA is used when there is a qualitative variable Y (with several modalities) and set of quantitative variables X. The aim was to find explicative factors for Y, and to predict Y modality knowing X values. In this paper, Y modalities correspond to CRK1 model and CRK2 model and X values represent selected physico-chemical properties of the 43 studied micropollutants.

3.7. Method for model comparisons

All the obtained CF_{HLB} and $CF_{membrane}$ curves were fitted with the CRK1 model first. If the determination coefficient (R^2) was ≥0.990, the CRK1 model was assigned. If not, the curves were then fitted with the CRK2 model which was considered to be the best kinetic model if the k_{u2} was confirmed to be significantly different than 0 based on a student *t*-test ($p < 0.05$). Otherwise, the CRK1 model was assigned even though its R^2 was <0.990. Moreover, if the k_{u2} term was significantly different from 0 but the resulting distribution coefficient of Eq. (8) (K_{HLB1} or $K_{membrane1}$) was negative or equal to 0, the CRK1 model was chosen.

4. Results and discussion

4.1. Identification of the best fitting model for accumulation of the 43 micropollutants

The CF_{HLB} uptake curves obtained previously (Morin et al., 2013) were tested to see if they belong to CRK1 model (Eq. (6)) or CRK2 model (Eq. (8)), as well as the 43 $CF_{membrane}$ as described above. Results are shown in Table 2, alongside the 28-day CF_{HLB} and the 28-day $CF_{membrane}$ data. The details for model classification are reported in the Supporting Information (SI) Tables S1 and S2, and the best fitting models for both the POCIS HLB phase and POCIS membrane are plotted in the SI, in Figs. S1 and S2, respectively. Micropollutants in these tables are classified according to their formerly attributed group in Morin et al. (2013) (based on a visual assessment of the data), and by increasing log D_{ow} (i.e. the ion-corrected octanol-water distribution coefficient). Coefficient log D_{ow} is calculated as follows:

$$\text{For acids}: \ \log D_{ow} = \log K_{ow} - \log\left(1 + 10^{pH-pKa}\right) \quad (11)$$

$$\text{For bases}: \ \log D_{ow} = \log K_{ow} - \log\left(1 + 10^{pKa-pH}\right) \quad (12)$$

As presented at the bottom of Table 2 (group 2), among the 13 micropollutants identified visually by Morin et al. (2013) with an inflexion point during kinetic accumulation in the POCIS HLB phase, the CRK2 model was confirmed to be the best kinetic model, with k_{u2} being significantly different from 0 (see Table S1).

Among the 30 micropollutants, at the top of Table 2 (group 1), visually identified by Morin et al. (2013) with a "classical" kinetic accumulation curve in the POCIS HLB phase (CRK1 model, Eq. (6)), 23 exhibited a $R^2 \geq 0.990$ (see Table S1). For the 7 micropollutants with $R^2 < 0.990$, the Student *t*-test indicated that the k_{u2} term in the CRK2 model fit was not significantly different from 0 (see Table S1). Thus, the CRK2 model was

Table 2
Identification of CRK1 or CRK2 model for the 43 micropollutants studied in the POCIS HLB phase and in the POCIS membrane and their respective concentration factors (CF_{HLB} and $CF_{membrane}$).

Conclusions from Morin et al. (2013)	Micropollutant	log D_{ow} (pH = 7.6)/ log K_{ow}[a]	Best kinetic model for the POCIS HLB phase	Best kinetic model for the POCIS membrane	28-day CF_{HLB} (L/g) ± standard deviation (n = 3)	28-day $CF_{membrane}$ (L/g) ± standard deviation (n = 3)
Group 1: accumulation curves without inflexion point (CRK1 model)	Tim	−0.82/1.34	CRK1	CRK1	16.97 ± 3.82	0.02 ± 0.00
	Ace	−0.44/1.53	CRK1	CRK1	12.94 ± 2.78	0.03 ± 0.00
	Met	−0.31/1.76	CRK1	CRK1	17.81 ± 5.31	0.08 ± 0.01
	Oxp	0.01/2.17	CRK1	CRK1	14.98 ± 3.88	0.07 ± 0.01
	Bis	0.13/2.20	CRK1	CRK1	14.98 ± 3.10	0.10 ± 0.01
	Bet	0.47/2.54	CRK1	CRK1	18.18 ± 4.73	0.73 ± 0.17
	Prop	0.51/2.58	CRK1	No CRK[b]	11.60 ± 3.03	1.63 ± 0.25
	Diclof	0.66/4.26	CRK1	CRK1	28.65 ± 5.48	0.35 ± 0.07
	Atra	2.20/2.20	CRK1	CRK1	27.02 ± 6.61	0.69 ± 0.02
	3.4-D[c]	2.35/2.35	CRK1	CRK1	31.79 ± 13.46	65.12 ± 6.00
	2,4-DCP[c]	2.49/2.88	CRK1	CRK1	5.05 ± 1.95	2.14 ± 0.19
	Diu[c]	2.53/2.53	CRK1	CRK1	25.74 ± 5.53	10.21 ± 1.39
	Lin[c]	2.68/2.68	CRK1	CRK1	19.41 ± 2.33	16.23 ± 2.24
	Carba	2.77/2.77	CRK1	CRK1	27.63 ± 6.16	0.25 ± 0.03
	Oxa	2.92/2.92	CRK1	CRK2	26.27 ± 5.58	0.28 ± 0.04
	t-BP[c]	3.21/3.21	CRK1	CRK2	35.37 ± 19.16	2.19 ± 0.48
	T	3.37/3.37	CRK1	CRK1	32.54 ± 5.84	0.30 ± 0.04
	Acet	3.50/3.50	CRK1	CRK1	26.53 ± 5.23	0.52 ± 0.02
	Lora	3.53/3.53	CRK1	CRK2	26.48 ± 5.45	0.39 ± 0.02
	Ala	3.59/3.59	CRK1	CRK2	25.97 ± 5.11	0.62 ± 0.02
	Pro[c]	3.62/3.62	CRK1	CRK1	28.18 ± 3.39	8.51 ± 1.21
	MegA[c]	3.72/3.72	CRK1	CRK1	35.60 ± 2.32	3.98 ± 0.38
	a-E2[c]	3.75/3.75	CRK1	CRK2	31.85 ± 3.70	1.26 ± 0.16
	b-E2[c]	3.75/3.75	CRK1	CRK1	29.39 ± 2.37	1.21 ± 0.15
	EE2[c]	3.90/3.90	CRK1	CRK2	35.56 ± 3.15	5.65 ± 0.72
	BPA[c]	4.04/4.04	CRK1	CRK1	34.37 ± 4.54	2.41 ± 0.27
	P[c]	4.15/4.15	CRK1	CRK1	51.08 ± 9.01	3.30 ± 0.31
	E1[c]	4.31/4.31	CRK1	CRK2	29.86 ± 3.70	1.69 ± 0.22
	t-OP[c]	4.69/4.69	CRK1	CRK2	10.79 ± 1.43	1.05 ± 0.05
	4-MBC[c]	5.12/5.12	CRK1	CRK1	30.27 ± 3.12	18.40 ± 2.86
Group 2: accumulation curves with an inflexion point (CRK2 model)	2.4-D acid	−2.29/2.50	CRK2	CRK1	5.52 ± 1.06	0.02 ± 0.00
	Sot	−2.24/−0.40	CRK2	CRK1	6.75 ± 1.96	0.00 ± 0.00
	Ate	−1.64/0.43	CRK2	CRK1	4.37 ± 1.13	0.00 ± 0.00
	Furo	−1.60/1.75	CRK2	CRK1	19.12 ± 4.88	0.11 ± 0.02
	Nad	−1.29/0.87	CRK2	No CRK[b]	13.34 ± 3.74	0.00 ± 0.00
	Napro	−0.42/2.99	CRK2	CRK1	13.79 ± 5.39	0.09 ± 0.01
	Keto	−0.11/3.61	CRK2	CRK1	19.26 ± 5.00	0.08 ± 0.01
	Beza	0.22/3.99	CRK2	CRK1	20.87 ± 5.71	0.08 ± 0.01
	Sulfa	0.52/0.79	CRK2	No CRK[b]	6.82 ± 1.57	0.00 ± 0.00
	Ibu	1.09/3.84	CRK2	No CRK[b]	21.05 ± 5.57	0.05 ± 0.01
	Trim	1.15/1.28	CRK2	CRK1	21.77 ± 6.12	0.06 ± 0.01
	Carb	1.80/1.80	CRK2	CRK1	23.50 ± 8.30	1.44 ± 0.06
	E3	2.67/2.67	CRK2	CRK1	26.80 ± 6.20	0.10 ± 0.01

[a] Source: http://www.chemicalize.com
[b] No CRK model chosen for the POCIS membrane as the software could not fit the data.
[c] Micropollutant with lag time for uptake in the POCIS HLB phase.

not chosen and the preferred model was CRK1. Therefore, the visual classification obtained previously (Morin et al., 2013) followed the statistical one obtained here.

Fitting of CRK1 or CRK2 models to the $CF_{membrane}$ data using the same statistical discrimination than with the POCIS HLB phase indicated that 8 micropollutants out of 43 showed an accumulation with an inflexion point (i.e. Oxa, t-BP, Lora, Ala, a-E2, EE2, E1 and t-OP; data shown in the SI, Figs. S1 and S2). For 4 molecules (Prop, Nad, Sulfa and Ibu), no model was preferred since the software could not fit the data properly. The 31 other micropollutants followed a first-order kinetic uptake in the membrane (CRK1 model). As the equilibrium was reached after 28 days in the membrane for these 31 micropollutants, the 28-day $CF_{membrane}$ corresponds to the membrane-water distribution coefficient K_{mp} or K_{mw}.

4.2. Influence of the POCIS membrane on the micropollutant accumulation

4.2.1. Visualization of membrane-controlled or HLB-controlled micropollutants

The Fig. 1 shows the relative proportion (expressed as a percentage) for each micropollutant between the concentration factor in the membrane after 7 days of exposure for the "pharmaceutical" POCIS ("pharmaceutical" POCIS 7-day $CF_{membrane}$) and the concentration factor in the membrane after 7 days of exposure for the "membrane-only" POCIS ("membrane_only" POCIS 7-day $CF_{membrane}$). In this experiment, the WBL control is not assessed, but this can be neglected as the two types of 7-day membrane are under the same experimental conditions.

As shown on Fig. 1, for the majority of the micropollutants studied, the 7-day $CF_{membrane}$ relative proportion of "pharmaceutical" POCIS to "membrane-only" POCIS was <100%. So, for the majority of the micropollutants considered, the POCIS HLB phase acted as a "sink" for the compounds sorbed in the membrane, and the flux into the whole "Pharmaceutical" POCIS was higher than into the "membrane-only" POCIS.

Few exceptions were observed, with a 7-day $CF_{membrane}$ relative proportion near 100%, for the following micropollutants with a CRK1 uptake model in the POCIS HLB phase: 3.4-D, 2.4-DCP, a-E2, b-E2, EE2 and BPA. This is also the case for the micropollutant Carb that follows a CRK2 uptake model in the POCIS HLB phase. For these compounds, membrane-resistance dominated uptake (limiting step) up to day 7 (either $\delta_m/(D_mK_{mw})$ or $\delta_p/(D_pK_{mp})$ dominated).

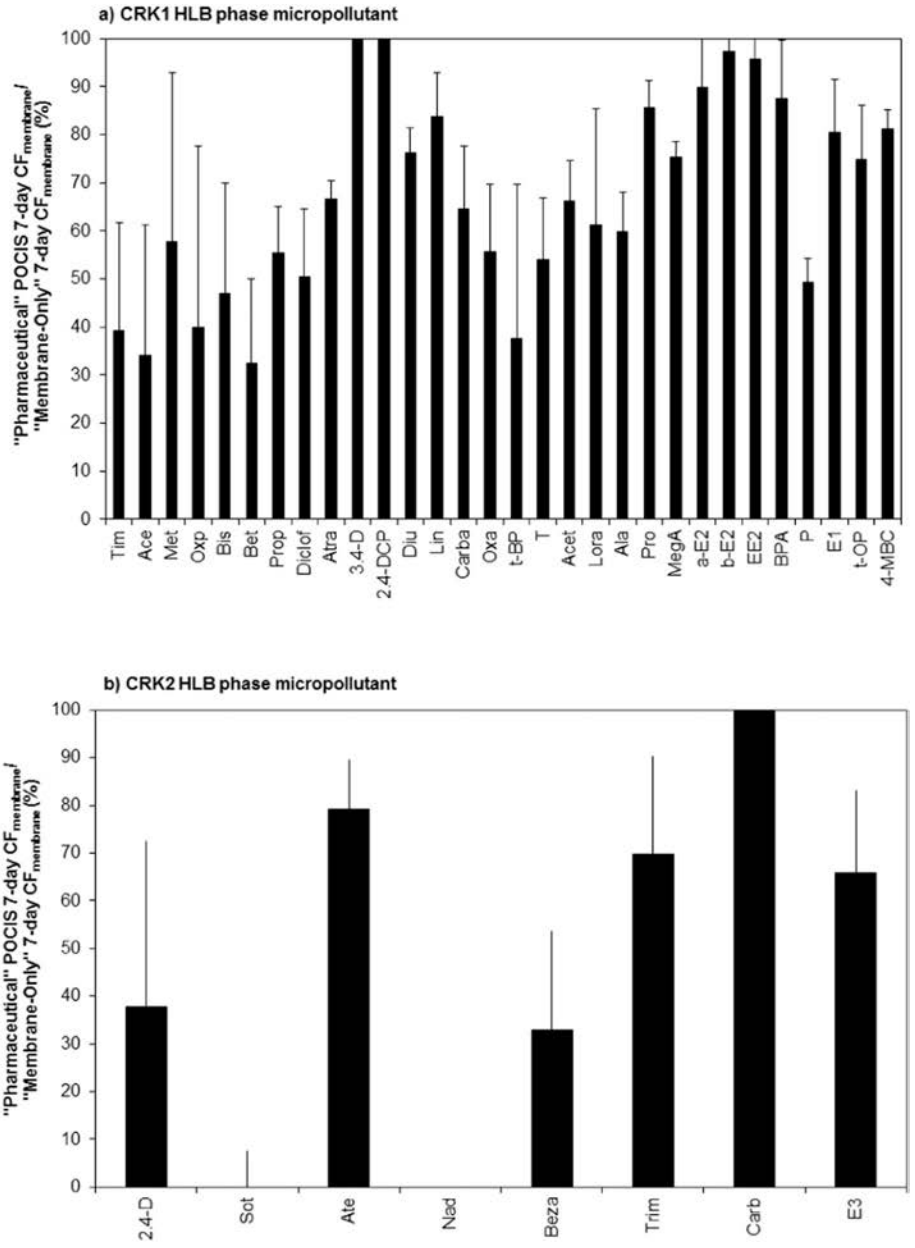


Fig. 1. Relative proportion (mean ± standard deviation, expressed as a percentage) of POCIS membrane concentration factors ($CF_{membrane}$) after 7 day exposure in the "Pharmaceutical" POCIS (with POCIS HLB phase; n = 3) relative to the "membrane-only" POCIS (without POCIS HLB phase; n = 3) for micropollutants with uptake best described using a) the CRK1 accumulation model for the POCIS HLB phase or b) the CRK2 accumulation model for the POCIS HLB phase. A y-axis value of 100% implies that $CF_{membrane}$ is identical using both types of POCIS. The data is organized from the smallest to largest log D_{OW} from the left to right side along the x-axis.

For the majority of compounds considered with $CF_{membrane}$ in "pharmaceutical" POCIS < $CF_{membrane}$ in the "membrane-only" POCIS, the micropollutants were either completely HLB-controlled ($\delta_{HLB}/(D_{HLB}K_{HLBm})$ or $\delta_{HLB}/(D_pK_{HLBp})$ dominated) or partially HLB-controlled. Hence, caution needs to be taken for interpretation of CRK2 model results presented in Fig. 1b, since all micropollutant POCIS membrane concentration factors, except for Carb, were very low (<1 L/g) leading to possible misinterpretations. For this reason, micropollutants for which relative proportion had high RSDs (>40%) (Furo, Ibu, Keto and Napro) or no accumulation in membrane (Sulfa), were not included in Fig. 1b.

A key finding from Table 2 and Fig. 1 is that it is not possible to directly deduce whether a micropollutant will exhibit CRK1 or CRK2 model in the POCIS HLB phase simply based on its affinity for the POCIS membrane or the POCIS HLB phase, as CRK1 or CRK2 model in the POCIS HLB phase can occur either for membrane or HLB dominated systems.

4.2.2. Changes in membrane-HLB distribution with time

To better understand the influence of the membrane on uptake model, we quantified micropollutant concentrations both in the POCIS membrane and in the POCIS HLB phase as a function of time. Four examples of micropollutant distribution between the POCIS membrane and the POCIS HLB phase are illustrated in Fig. 2. Results for all micropollutants are presented in Fig. S1 (for CRK1 model in the POCIS HLB phase) and Fig. S2 (for CRK2 model in the POCIS HLB phase) in the SI.

Fig. 2a, for Ate, is illustrative of both negligible accumulation into the POCIS membrane and CRK2 POCIS HLB phase uptake model. In this case, the global resistance to the mass transfer is probably dominated by the HLB sorbent. Fig. 2b, for Carb, is illustrative of CRK2 POCIS HLB phase uptake model, with a likely membrane control (over the sorbent), since both significant accumulation into this compartment and relative proportion of 100% for the POCIS $CF_{membrane}$ (Fig. 1b) were observed. Fig. 2c, for Ace, illustrates behaviour of CRK1 POCIS HLB phase uptake

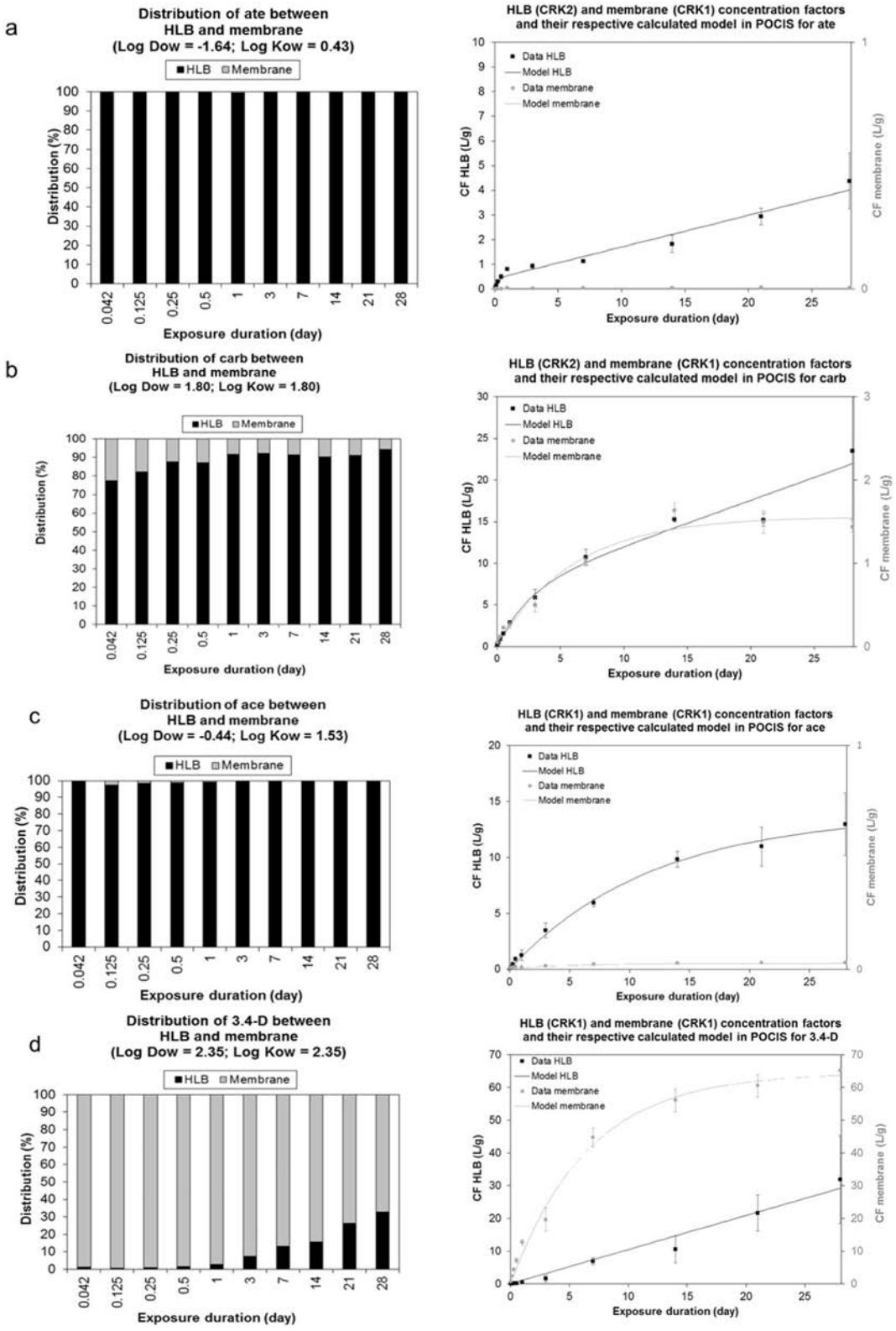


Fig. 2. Relative distribution between the POCIS HLB phase and the membrane (left side) and concentration factors (CF) in POCIS HLB phase and in membrane (right side) as a function of the time for CRK2 model POCIS HLB phase micropollutants (atenolol (a.), carbendazim (b.) and CRK1 model POCIS HLB phase micropollutants (acebutolol (c.) and 3.4-dichloroaniline (d.). Results for the membrane in grey and for the POCIS HLB phase in black (n = 3). CF determination explained in Section 3.3.

model in which the HLB phase dominates uptake. And Fig. 2d, for 3.4 D, illustrates behaviour of CRK1 POCIS HLB phase uptake model in which the membrane dominates uptake. Fig. 2 also shows that the micropollutants studied could have a CRK1 or CRK2 uptake model in the POCIS HLB phase, whether the compounds are substantially accumulated in the membrane ($CF_{membrane}$ > 1 L/g) or not (see also Table 1 and Figs. S1 and S2). Note that the CRK1 or the CRK2 uptake model observed in the POCIS HLB phase only explains the main accumulation

mechanism in the sorbent. Other minor mechanisms could occur even though they are not visualized on the kinetic curve of accumulation.

The hypothesis proposed in the introduction of this paper that membrane plays a contributing role on whether uptake in the POCIS HLB phase follows a CRK1 or CRK2 model was not confirmed for all studied compounds. The accumulation in the POCIS membrane could follow a CRK1 or CRK2 model, this had no consistent impact on the type of accumulation in the POCIS HLB phase (see Figs. S1 and S2). It is probably due to the fact that the micropollutants diffuse through the membrane pores anyway (Alvarez et al., 2004; Kaserzon et al., 2014; Booij et al., 2017). Nevertheless, a high accumulation in the membrane ($CF_{membrane}$ ≥ 2 L/g) will lead to a lag time in the POCIS HLB phase, probably due to a double mechanism of interaction with the membrane: through the membrane water-filled pores on the one hand and through the PES matrix on the other hand (Fig. 2d and Table 1). But, it should be taken into account that all micropollutants following a CRK2 model for the POCIS HLB phase accumulated poorly in the membrane (28-day $CF_{membrane}$ < 1 L/g), except for Carb.

It is also evident for several micropollutants that sorption to POCIS membrane generally occurred in two stages: a rapid increase on the initial day of exposure, followed by a slower increase in uptake (see for example Bet, Atra, Carba in Fig. S1). This indicates a two-phase kinetic for the POCIS membrane, often giving the appearance of a CRK2 model uptake for the membrane. This could be due to initial and fast transfer through the membrane pores (bulk phase as well as micropores), followed by a slower sorption into PES polymer. The POCIS HLB phase seemed to display a similar behaviour for some micropollutants, as illustrated for Ate (Fig. 2a). Such a two-stage kinetics was also recently reported for static uptake of 54 PCBs in polyoxymethylene (POM) passive samplers (Arp et al., 2015).

4.2.3. Role of micropollutant properties

The accumulation in POCIS membrane depends partly on the micropollutant hydrophobicity and ionization. Indeed, as shown on Table 1, micropollutants with log D_{ow} < 2.3 did not accumulate significantly (28-day $CF_{membrane}$ < 1 L/d; 19 micropollutants out of 21), while micropollutants with log D_{ow} > 3.6 accumulated significantly (28-day $CF_{membrane}$ ≥ 1 L/d; 10 micropollutants out of 10), and were characterized by a lag time in the POCIS HLB phase. Between those values (log D_{ow} from 2.3 to 3.6), only micropollutants having 2 or 3 chlorines substituted on the same phenyl group were significantly retained in the POCIS membrane (5 micropollutants out of 5). Those micropollutants were also characterized by lag times for the POCIS HLB phase. It is possible that chlorine atoms substituted on the same phenyl groups have particular affinity for PES membranes.

These results are in agreement with those of Vermeirssen et al. (2012), who observed higher accumulations in PES membrane of "pesticide" POCIS with increasing micropollutant hydrophobicity (among pharmaceuticals and pesticides in an effluent wastewater treatment plant).

4.3. Is it possible to predict the accumulation model in the POCIS HLB phase for a new micropollutant?

We performed a FDA analysis ($\alpha = 0.05$) to study the accumulation model (CRK1 or CRK2 model) of the 43 target micropollutants in the POCIS HLB phase, after passing through the POCIS membrane. We tested some of the physico-chemical properties used to predict the "druglikeness" of a compound (i.e., its ability to pass through biological layers and to bind to a specific ligand) (e.g. Veber et al., 2002), or its chromatographic retention times (e.g. Bade et al., 2015). We considered octanol-water distribution coefficient, ionization state, molar mass, polarisability, polar surface area and apolar surface area. We also tested the volume of the compound, its projection area, its aromatic bounds and its pi-energy. All these physico-chemical properties are compiled in Table S3. They were obtained from a single database (www.chemicalize.com) to use homogenised values (as example, log K_{ow} values can be variable from one source to another). These properties describe the hydrophobic-hydrophilic character of the molecule (log D_{ow}, aromatic bounds), polar interactions (number of oxygen, nitrogen and hydrogen-bonding atoms defined by the polar surface area, PSA), apolar interactions (apolar surface area, ASA), ionization, size (volume and projection area), molar mass, polarizability and ∏ electron (pi energy) organization.

Qualitativep variables were based on three groups: Group 1L) CRK1 model in POCIS HLB phase with linear accumulation ($t_{1/2}$ > 14 days); Group 1C) CRK1 model in POCIS HLB phase with curvilinear accumulation ($t_{1/2}$ lower than 14 days); Group 2) CRK2 model in POCIS HLB phase (see on Fig. 3 the illustration of the FDA analysis).

The representation of variables indicates that log D_{ow}, ionization (included in log D_{ow}) and polar surface area were the main variables explaining the total variance (Fig. 3a). To a lesser extent, pi energy, projection area and apolar surface area also had some influence.

The representation of observations indicates that Group 1L (CRK1; $t_{1/2}$ > 14) was positively correlated with log D_{ow}, projection area and apolar surface area and negatively correlated with ionization, pi energy and polar surface area (Fig. 3b). Thus, Group 1L micropollutants tended to be more hydrophobic. Indeed, as detailed on Table S1, these molecules are generally neutral and have log D_{ow} > 2.5, PSA < 50 Å^2, ASA > 380 Å^2, pi energy <25 β and projection area > 40 Å^2.

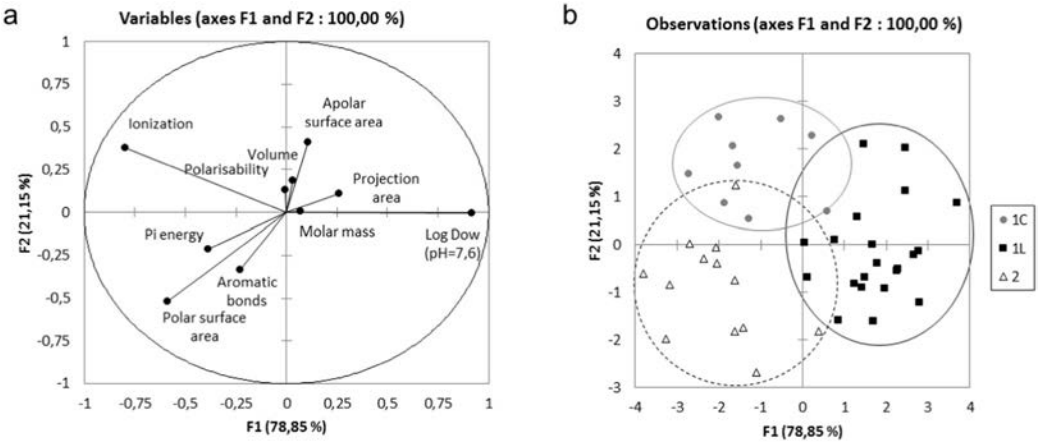


Fig. 3. Factorial discriminant analysis (FDA) indicating a) variables of physico-chemical properties of the studied micropollutants and b) observations of the CRK1L (black squares), CRK1C (grey circles) and CRK2 (white triangles) modalities of uptake into the HLB phase of "pharmaceutical" POCIS.

Also, Group 1C (CRK1; $t_{1/2} < 14$) was positively correlated with ionization, polar surface area, pi energy and apolar surface area; but anti-correlated with log D_{ow} and projection area (Fig. 3b). These molecules interact mainly with ionic interactions and possibly through pi-pi interactions. They are generally characterized by log $D_{ow} < 2.5$, PSA < 50 Å^2, ASA > 380 Å^2, pi energy ≈ 25 β and projection area < 40–45 Å^2.

Group 2 (CRK2) was positively correlated with ionization, polar surface area, pi energy; but negatively correlated with log D_{ow}, projection area and apolar surface area. This suggests that interactions with the POCIS HLB phase occurred through polar and ionic interactions, but also pi-pi interactions. These molecules have generally log $D_{ow} < 2.5$, PSA > 50 Å^2, ASA < 380 Å^2, pi energy > 25 β and projection area < 40 Å^2 (Table S1).

So, the FDA permitted to classify micropollutants in the 3 groups, 1L, 1C and 2, with >90% confidence. According to the same FDA, but considering only the two most important variables (log D_{ow} and PSA), this confidence was still above 70%. This indicates that the accumulation model (CRK1 or CRK2 model) could be estimated only with the hydrophobic-hydrophilic and polar characters of a micropollutant. Micropollutants that would accumulate in the POCIS HLB phase according to a CRK1 model would have log $D_{ow} > 2.5$ and PSA < 50 Å^2; while micropollutants with log $D_{ow} < 2.5$ and PSA > 50 Å^2 would follow a CRK2 model in the POCIS HLB phase (70% confidence).

To our knowledge, this is the first study with identification of the most suitable physico-chemical properties for predicting the micropollutant accumulation model in the POCIS HLB phase. Miller et al. (2016) achieved a similar prediction study in the aim to determine sampling rates (without considering kinetic model of accumulation). Interestingly, their conclusions are consistent with ours. Firstly, performing a genetic algorithm model, they showed that log D_{ow} induced the highest correlations between predicted and measured R_s, and they noticed that it was insufficient to describe sorption to POCIS sorbents. Secondly, using a chromatographic retention model, they identified as major physico-chemical descriptors: log D_{ow}, benzene rings, number of five- or nine-membered rings, as well as number of carbons, oxygens or hydrophilic factor. Except the five- or nine-membered rings, we tested the same physico-chemical descriptors as Miller et al. (2016) (considering that benzene rings is included in aromatic rings; number of carbons, oxygens and hydrophilic factor are included in apolar surface area, polar surface area and log D_{ow}).

5. Conclusions

This study is the first resulting in 1) micropollutants accumulation kinetics and models in the POCIS membrane over a 28-day period; 2) membrane-water distribution coefficients (K_{mw} or K_{mp}) for 31 micropollutants; 3) the influence of the membrane leading to lag times in the POCIS HLB phase for the micropollutants characterized by a strong affinity for the membrane ($CF_{membrane} > 2$ L/g); 4) the identification of the micropollutant uptake control by the POCIS membrane or the POCIS HLB phase determined by analyses of POCIS membrane exposed with and without POCIS HLB phase; 5) the prediction of the CRK1 or CRK2 accumulation model, using a factorial discriminant analysis, with >90% confidence; and the identification of log D_{ow} and polar surface area as the most influent parameters to predict the type of accumulation model of micropollutants.

Further experiments with longer exposure durations of POCIS might allow a better understanding of the CRK2 model for the POCIS HLB phase, as the equilibrium regime was never reached in this work for 28-days exposure for the target micropollutants.

This work contributes to better predict when a micropollutant will undergo a CRK1 or CRK2 uptake model in the POCIS HLB phase. This will allow the use of more accurate model to calculate more reliable uptake rates.

We showed that only a subset of 30 target micropollutants exhibited the simplest model of uptake in the POCIS HLB phase, CRK1, which could be a pre-requisite for isotropic mechanisms between PRC desorption and micropollutant sorption. For micropollutants with CRK2 model in the POCIS HLB phase, the use of PRC is not appropriate and cannot allow correcting sampling rates for environmental conditions because of anisotropic adsorption and desorption mechanisms. Since there is currently no suitable strategy of R_s correction for these last micropollutants, POCIS and other adsorption-based tools were recently considered as passive samplers leading to TWA concentrations with unknown uncertainties (Miège et al., 2015).

Acknowledgments

The authors thank the Cluster de Recherche Rhône-Alpes Environnement for financing Nicolas Morin's thesis and the MEEDM (Ministère de l'Ecologie, de l'Environnement, du Développement durable et de la Mer) for financing Julien Camilleri's thesis. Hans Peter H. Arp's contribution benefited from the NGI sabbatical fund (grant 12116).

References

Alvarez, D.A., 1999. Development of an Integrative Sampling Device for Hydrophilic Organic Contaminants in Aquatic Environments. University of Missouri-Columbia, Columbia, MO, USA.

Alvarez, D.A., Petty, J.D., Huckins, J.N., Jones-Lepp, T.L., Getting, D.T., Goddard, J.P., Manahan, S.E., 2004. Development of a passive, in situ, integrative sampler for hydrophilic organic contaminants in aquatic environments. Environ. Toxicol. Chem. 23 (7), 1640–1648.

Alvarez, D.A., Stackelberg, P.E., Petty, J.D., Huckins, J.N., Furlong, E.T., Zaugg, S.D., Meyer, M.T., 2005. Comparison of a novel passive sampler to standard water-column sampling for organic contaminants associated with wastewater effluents entering a New Jersey stream. Chemosphere 61 (5), 610–622.

Arp, H.P.H., Hale, S.E., Elmquist Kruså, M., Cornelissen, G., Grabanski, C.B., Miller, D.J., Hawthorne, S.B., 2015. Review of polyoxymethylene passive sampling methods for quantifying freely dissolved porewater concentrations of hydrophobic organic contaminants. Environ. Toxicol. Chem. 34 (4), 710–720.

Bade, R., Bijlsma, L., Miller, T.H., Barron, L.P., Sancho, J.V., Hernández, F., 2015. Suspect screening of large numbers of emerging contaminants in environmental waters using artificial neural networks for chromatographic retention time prediction and high resolution mass spectrometry data analysis. Sci. Total Environ. 538, 934–941.

Bäuerlein, P.S., Mansell, J.E., Ter Laak, T.L., De Voogt, P., 2012. Sorption behavior of charged and neutral polar organic compounds on solid phase extraction materials: which functional group governs sorption? Environ. Sci. Technol. 46 (2), 954–961.

Belles, A., Pardon, P., Budzinski, H., 2014a. Development of an adapted version of polar organic chemical integrative samplers (POCIS-Nylon). Anal. Bioanal. Chem. 406 (4), 1099–1110.

Belles, A., Tapie, N., Pardon, P., Budzinski, H., 2014b. Development of the performance reference compound approach for the calibration of "polar organic chemical integrative sampler" (POCIS). Anal. Bioanal. Chem. 406 (4), 1131–1140.

Booij, K., Sleiderink, H.M., Smedes, F., 1998. Calibrating the uptake kinetics of semipermeable membrane devices using exposure standards. Environ. Toxicol. Chem. 17 (7), 1236–1245.

Booij, K., Hofmans, H.E., Fischer, C.V., Van Weerlee, E.M., 2003. Temperature-dependent uptake rates of nonpolar organic compounds by semipermeable membrane devices and low-density polyethylene membranes. Environ. Sci. Technol. 37 (2), 361–366.

Booij, K., Maarsen, N.L., Theeuwen, M., Van Bommel, R., 2017. A method to account for the effect of hydrodynamics on polar organic compound uptake by passive samplers. Environ. Toxicol. Chem. 36 (6), 1517–1524.

Camilleri, J., Morin, N., Miège, C., Coquery, M., Cren-Olivé, C., 2012. Determination of the uptake and release rates of multifamilies of endocrine disruptor compounds on the polar C18 Chemcatcher. Three potential performance reference compounds to monitor polar pollutants in surface water by integrative sampling. J. Chromatogr. A 1237, 37–45.

Carlson, J.C., Challis, J.K., Hanson, M.L., Wong, C.S., 2013. Stability of pharmaceuticals and other polar organic compounds stored on polar organic chemical integrative samplers and solid-phase extraction cartridges. Environ. Toxicol. Chem. 32 (2), 337–344.

Fauvelle, V., Mazzella, N., Delmas, F., Madarassou, K., Eon, M., Budzinski, H., 2012. Use of mixed-mode ion exchange sorbent for the passive sampling of organic acids by polar organic chemical integrative sampler (POCIS). Environ. Sci. Technol. 46 (24), 13344–13353.

Fauvelle, V., Mazzella, N., Belles, A., Moreira, A., Allan, I.J., Budzinski, H., 2014. Optimization of the polar organic chemical integrative sampler for the sampling of acidic and polar herbicides. Anal. Bioanal. Chem. 406 (13), 3191–3199.

Gabet-Giraud, V., Miège, C., Choubert, J.-M., Martin-Ruel, S., Coquery, M., 2010. Analysis of estrogens and beta blockers in the dissolved phase of wastewater treatment plants in France. Sci. Total Environ. 408, 4257–4269.
Górecki, T., Namienik, J., 2002. Passive sampling. TrAC Trends Anal. Chem. 21 (4), 276–291.
Górecki, T., Yu, X., Pawliszyn, J., 1999. Theory of analyte extraction by selected porous polymer SPME fibres. Analyst 124 (5), 643–649.
Harman, C., Allan, I.J., Bäuerlein, P.S., 2011. The challenge of exposure correction for polar passive samplers the PRC and the POCIS. Environ. Sci. Technol. 45 (21), 9120–9121.
Huckins, J.N., Manuweera, G.K., Petty, J.D., Mackay, D., Lebo, J.A., 1993. Lipid-containing semipermeable membrane devices for monitoring organic contaminants in water. Environ. Sci. Technol. 27 (12), 2489–2496.
Huckins, J.N., Petty, J.D., Orazio, C.E., Lebo, J.A., Clark, R.C., Gibson, V.L., Gala, W.R., Echols, K.R., 1999. Determination of uptake kinetics (sampling rates) by lipid-containing semipermeable membrane devices (SPMDs) for polycyclic aromatic hydrocarbons (PAHs) in water. Environ. Sci. Technol. 33 (21), 3918–3923.
Huckins, J.N., Petty, J.D., Lebo, J.A., Almeida, F.V., Booij, K., Alvarez, D.A., Cranor, W.L., Clark, R.C., Mogensen, B.B., 2002. Development of the permeability/performance reference compound approach for in situ calibration of semipermeable membrane devices. Environ. Sci. Technol. 36 (1), 85–91.
Huckins, J.N., Petty, J.D., Booij, K. (Eds.), 2006. Monitors of Organic Chemicals in the Environment: Semipermeable Membrane Devices. Springer.
Kaserzon, S.L., Hawker, D.W., Kennedy, K., Bartkow, M., Carter, S., Booij, K., Mueller, J.F., 2014. Characterisation and comparison of the uptake of ionizable and polar pesticides, pharmaceuticals and personal care products by POCIS and Chemcatchers. Environ. Sci.: Processes Impacts 16 (11), 2517–2526.
Lissalde, S., Mazzella, N., Fauvelle, V., Delmas, F., Mazellier, P., Legube, B., 2011. Liquid chromatography coupled with tandem mass spectrometry method for thirty-three pesticides in natural water and comparison of performance between classical solid phase extraction and passive sampling approaches. J. Chromatogr. A 1218 (11), 1492–1502.
Mazzella, N., Dubernet, J.F., Delmas, F., 2007. Determination of kinetic and equilibrium regimes in the operation of polar organic chemical integrative samplers. Application to the passive sampling of the polar herbicides in aquatic environments. J. Chromatogr. A 1154 (1–2), 42–51.
Miège, C., Bados, P., Brosse, C., Coquery, M., 2009. Method validation for the analysis of estrogenic hormones (including conjugated compounds) in various aqueous matrices. Trends Anal. Chem. 28 (2), 237–244.
Miège, C., Mazzella, N., Allan, I., Dulio, V., Smedes, F., Tixier, C., Vermeirssen, E., Brant, J., O'Toole, S., Budzinski, H., Ghestem, J.P., Staub, P.F., Lardy-Fontan, S., Gonzalez, J.L., Coquery, M., Vrana, B., 2015. Position paper on passive sampling techniques for the monitoring of contaminants in the aquatic environment - achievements to date and perspectives. Trends in Environ. Anal. Chem. 8, 20–26.
Miller, T.H., Baz-Lomba, J.A., Harman, C., Reid, M.J., Owen, S.F., Bury, N.R., Thomas, K.V., Barron, L.P., 2016. The first attempt at non-linear in silico prediction of sampling rates for polar organic chemical integrative samplers (POCIS), 2016. Environ. Sci. Technol. 50, 7973–7981.
Mills, G.A., Gravell, A., Vrana, B., Harman, C., Budzinski, H., Mazzella, N., Ocelka, T., 2014. Measurement of environmental pollutants using passive sampling devices - an updated commentary on the current state of the art. Environ. Sci.: Processes Impacts 16 (3), 369–373.
Morin, N., Miège, C., Coquery, M., Randon, J., 2012. Chemical calibration, performance, validation and applications of the polar organic chemical integrative sampler (POCIS) in aquatic environments. TrAC Trends Anal. Chem. 36, 144–175.
Morin, N., Camilleri, J., Cren-Olive, C., Coquery, M., Miege, C., 2013. Determination of uptake kinetics and sampling rates for 56 organic micropollutants using "pharmaceutical" POCIS. Talanta 109, 61–73.
Rafferty, J.L., Zhang, L., Siepmann, J.I., Schure, M.R., 2007. Retention mechanism in reversed-phase liquid chromatography: a molecular perspective. Anal. Chem. 79 (17), 6551–6558.
Rusina, T.P., Smedes, F., Koblizkova, M., Klanova, J., 2010. Calibration of silicone rubber passive samplers: experimental and modeled relations between sampling rate and compound properties. Environ. Sci. Technol. 44 (1), 362–367.
Seethapathy, S., Górecki, T., Li, X., 2008. Passive sampling in environmental analysis. J. Chromatogr. A 1184 (1–2), 234–253.
Veber, D.F., Johnson, S.R., Cheng, H.-Y., Smith, B.R., Ward, K.W., Kopple, K.D., 2002. Molecular properties that influence the oral bioavailability of drug candidates. J. Med. Chem. 45, 2615–2623.
Vermeirssen, E.L.M., Körner, O., Schönenberger, R., Suter, M.J.F., Burkhardt-Holm, P., 2005. Characterization of environmental estrogens in river water using a three pronged approach: active and passive water sampling and the analysis of accumulated estrogens in the bile of caged fish. Environ. Sci. Technol. 39 (21), 8191–8198.
Vermeirssen, E.L.M., Dietschweiler, C., Escher, B.I., Van Der Voet, J., Hollender, J., 2012. Transfer kinetics of polar organic compounds over polyethersulfone membranes in the passive samplers POCIS and Chemcatcher. Environ. Sci. Technol. 46 (12), 6759–6766.
Vrana, B., Allan, I.J., Greenwood, R., Mills, G.A., Dominiak, E., Svensson, K., Knutsson, J., Morrison, G., 2005. Passive sampling techniques for monitoring pollutants in water. TrAC Trends Anal. Chem. 24 (10), 845–868.
Zabiegała, B., Kot-Wasik, A., Urbanowicz, M., Namieśnik, J., 2010. Passive sampling as a tool for obtaining reliable analytical information in environmental quality monitoring. Anal. Bioanal. Chem. 396 (1), 273–296.